Acta metall. mater. Vol. 38, No. 4, pp. 671–683, 1990
Printed in Great Britain.

0956-7151/90 $3.00 + 0.00

A NEW MODEL-BASED CREEP EQUATION FOR DISPERSION STRENGTHENED MATERIALS

J. RÖSLER† and E. ARZT‡

Max-Planck-Institut für Metallforschung, Seestraße 92, D-7000 Stuttgart 1, F.R.G.

(*Received* 7 *June* 1989)

Abstract—The strongly stress-sensitive and temperature-dependent creep behaviour of dispersion strengthened materials cannot be described satisfactorily by current creep laws. In this paper a new creep equation is developed which considers as the rate-controlling event the thermally activated detachment of dislocations from dispersoid particles exerting an attractive force. The approach is motivated by recent TEM observations and theoretical calculations which strongly suggest that the "classical" view, according to which particles merely force dislocations to climb around them, is inadequate. The creep equation is applied to a dispersion-strengthened superalloy, two aluminium alloys and bubble-strengthened tungsten. Practical conclusions, regarding the optimum dispersoid size and alloy development, are drawn.

Résumé—Le fluage dépendant fortement de la contrainte et de la température sur des matériaux renforcés par dipersion ne peut être décrit d'une manière satisfaisante par les lois classiques du fluage. Dans cet article une nouvelle équation de fluage est développée: elle considère que l'évènement qui contrôle la vitesse de fluage est le détachement thermiquement activé des dislocations à partir des particules dispersées qui exercent une force attractive. L'approche est motivée par des observations récentes par MET et des calculs théoriques qui suggèrent fortement que l'idée "classique" selon laquelle les particules forcent simplement les dislocations à monter autour d'elles est inadaptée. L'équation de fluage est appliquée à un superalliage renforcé par dispersion, à deux alliages d'aluminium et au tungstène renforcé par bulles. On donne des conclusions pratiques, relatives à la taille optimale du dispersoïde et au développement de l'alliage.

Zusammenfassung—Das sehr spannungsempfindliche und temperaturabhängige Kriechverhalten von dispersionsgehärteten Werkstoffen kann mit den gängigen Kriechgesetzen nicht befriedigend beschrieben werden. In dieser Arbeit wird eine neue Gleichung für das Kriechen entwickelt. Diese geht aus von dem thermisch aktivierten Losreißen der Versetzungen von den dispergierten Teilchen, die eine attraktive Kraft ausüben, als dem geschwindigkeitsbestimmenden Schritt. Dieses Vorgehen wird durch neuere TEM-Untersuchungen und theoretische Berechnungen nahegelegt; danach ist die "klassische" Sicht, daß die Teilchen durch Klettern der Versetzungen überwunden werden, nicht richtig. Die Gleichung wird auf eine dispersionsgehärtete Superlegierung, zwei Aluminiumlegierungen und porengehärtetes Wolfram angewendet. Praktische Folgerungen werden im Hinblick auf die optimale Teilchengröße und die Legierungsentwicklung gezogen.

1. INTRODUCTION

Dispersion-strengthened alloys have a creep behaviour which in the light of current theoretical concepts can be characterized as "unusual": the stress sensitivity of the creep rate is almost always found to be extremely high, with stress exponents n well above 20 and sometimes as high as 100 extending over several decades in strain rate [1–8]—as opposed to dispersoid-free alloys for which usually $n \leqslant 10$. Also the activation energies for creep deformation of dispersion-strengthened materials are generally found to be "too" high, in some cases up to a factor of about three above the expected value (i.e. the activation energy for volume diffusion). While the exact reasons for this behaviour are not well understood, a formal representation of the creep data can be obtained with the following semi-empirical creep equation [9, 10]

$$\dot{\epsilon} = A \cdot \frac{D_v \cdot G \cdot b}{k_B T} \cdot \left(\frac{\sigma - \sigma_{th}}{G} \right)^n \qquad (1)$$

where $\dot{\epsilon}$ is the creep rate, σ the applied stress, D_v the diffusivity, G the shear modulus, b the Burgers vector, k_B Boltzmann's constant, T the absolute temperature, A a dimensionless constant and n the stress exponent. Compared to the conventional "power-law creep" equation [11], equation (1) contains a "threshold stress" σ_{th} below which creep deformation is assumed to be negligible. This assumption leads to an arbitrarily high apparent stress exponent on $\log \dot{\epsilon} - \log \sigma$ plots in the vicinity of σ_{th}. By curve fitting, consistent sets of values for σ_{th}, A and n can usually be found which enable equation (1) to describe the creep data within a certain range of experimental conditions.

The inadequacies of this parametric approach are however quite evident: the parameter σ_{th} is not a

†Present address: Materials Department, University of California, Santa Barbara, CA 93106, U.S.A.
‡Present address: Department of Materials Science and Engineering, Stanford University, Stanford, CA 94305, U.S.A.

good material constant as it often varies with both 672temperature and applied stress; this adds considerable uncertainty to extrapolations of creep rates into ranges where experimental data are not available. In view of the great potential of dispersion-strengthened alloys as high-performance materials this is a serious practical limitation of equation (1).

The inadequacy of this equation is accentuated by the fact that the physical foundation for a "threshold stress" σ_{th} is questionable from a scientific point-of-view (for a recent review see [8]). While it is well established that hard, non-shearable dispersoid particles impede room-temperature deformation below a well-defined yield stress (the Orowan stress [12]), the extension of the Orowan concept to higher temperatures (e.g. [13]) has not been successful. The reason lies in the ability of dislocations to circumvent obstacles, at high temperatures, by climb. Early models of this process [14, 15] have shown that such a mechanism leads merely to a retardation of creep by introducing "waiting times" for dislocations at the particles, without changing the stress dependence of the creep rate significantly. A "threshold stress" for dislocation climb was predicted by Brown and Ham [16] and Shewfelt and Brown [17], who note that the dislocation has to increase its line length in order to surmount the particle. The theoretical threshold stress, which would support the approach taken in equation (1), scales with the Orowan stress and is a function of particle shape. However, the peculiar dislocation geometry postulated by the authors ("local climb") has been criticized [18] and recent model calculations by the present authors [19] have shown that climb of dislocations with an "equilibrium shape" is rapid at high temperatures and does not lead to high stress exponents, nor to significant "threshold stresses". Thus dislocation climb alone appears to be insufficient as an explanation for the creep behaviour of dispersion-strengthened alloys.

An alternative possibility for the process controlling the creep rate of dispersion-strengthened materials lies in the existence of an attractive particle–dislocation interaction, as suggested by TEM studies of dislocation structures in crept specimens [20, 21, 6]. A typical micrograph from a detailed study by Schröder and Arzt [21] is reproduced in Fig. 1(a), where the dislocation is seen to be captured at the detachment side of the particle after climb has been completed. New results along similar lines have been reported in a recent, more quantitative study by Herrick *et al.* [22].

Support for the validity of these observations comes from theoretical studies by Srolovitz *et al.* [23, 24], who show that an attractive interaction between dislocations and incoherent particles would in fact be expected at high temperatures because the incoherent interface can relax parts of the dislocation's stress field by slipping and rapid diffusion. Furthermore, Arzt and Wilkinson [25] have calculated the energetics of dislocation climb over an attractive particle and found that dislocation detachment requires higher stresses than the even unlikely process of "local" climb, provided that the line energy of the dislocation is only moderately relaxed by the incoherent interface. From this energetic consideration one would expect a well-defined threshold stress caused by the detachment process, which would justify the use of equation (1). However, because of the special shape of the force–distance profile, dislocation detachment may be thermally activated, as suggested by Rösler and Arzt [6, 26]. Thus dislocation creep well below the athermal "threshold stress" may be possible under certain circumstances.

Table 1. Nomenclature

$\dot{\epsilon}$	creep rate
G	shear modulus
b	Burgers vector
D_v	volume diffusivity
Q_v	activation energy for volume diffusion
T	absolute temperature
k_B	Boltzmann's constant
σ_{th}	"threshold stress"
σ	stress
τ	shear stress
σ_0, τ_0	Orowan stress in tension and shear, respectively
σ_d, τ_d	athermal detachment stress in tension and shear, respectively [equation (10)]
n	stress exponent
n_{app}	"apparent" stress exponent [equation (21)]
Q_{app}	"apparent" activation energy for creep [equation (23)]
E_d	energy for dislocation detachment [equation (14)]
T_P, T_M	dislocation line energy at the particle and in the matrix, respectively
k	relaxation parameter [equation (3)]
r	characteristic particle dimension
2λ	particle spacing
ρ	density of mobile dislocations

In this paper we give a kinetic analysis of the detachment process which takes the effect of thermal activation into account. Depending upon the strength of the particle-dislocation interaction, significant deviations from a threshold-like behaviour [equation (1)] are predicted. Based on these calculations, a new creep equation of the form

$$\dot{\epsilon} = \dot{\epsilon}_0 \cdot \exp\left(\frac{E_d}{k_B T}\right) \tag{2}$$

is proposed, where E_d is the activation energy for the detachment process, and $\dot{\epsilon}_0$ a reference strain rate. The equation is derived in Sections 2 and 3, and its implications are then considered (Section 4). The model calculations are compared with experimental creep data in Section 5. The paper concludes with consequences for the optimum design of dispersion strengthened materials. The symbols used are listed in Table 1.

2. THE ACTIVATION ENERGY FOR DISLOCATION DETACHMENT

The first step is to analyze the energetics of dislocation detachment from an attractive dispersoid particle in order to arrive at an analytical expression for the detachment activation energy E_d. We consider the

passage of a dislocation through a uniform array of spherical particles of radius r and spacing 2λ and focus the previous line-tension analysis by Arzt and Wilkinson [25] (A–W) on the detachment process. As proposed by A–W, the attractive interaction is modelled by assuming that the line energy of the dislocation is lowered at the particle interface to a value given by

$$T_P = k \cdot T_M \tag{3}$$

where T_M is the line energy of the dislocation in the matrix, given to a reasonable approximation by $T_M = Gb^2/2$. The parameter k $(0 \leqslant k \leqslant 1)$ can be thought of as a relaxation parameter. For $k = 1$, no attraction between particle and dislocation exists; for $k < 1$, an attractive interaction results, which becomes *stronger* with *diminishing* k.

The process of dislocation detachment is illustrated schematically in Fig. 1(b). When, under the action of a shear stress τ, the dislocation moves an increment dx in the glide direction, two contributions to the change in internal energy have to be considered. The first energy term dU is due to the exchange of dislocation line length at the particle (with line energy $k \cdot T_M$) by line length in the matrix (with higher energy T_M). It amounts to (see A–W)

$$dU = \frac{2k \cdot T_M}{\sqrt{1-\left(\frac{a}{r}\right)^2}}\,da - \frac{2T_M}{\sqrt{1-(\tau/\tau_0)^2}} \cdot da \tag{4}$$

where a is given, as in the A–W analysis, by

$$a = \sqrt{r^2 - h^2 - x^2} \tag{5}$$

i.e. half the distance between the two points at which the dislocation contacts the particle [Fig. 1(b)]. h is the height-of-intersection of the glide plane above the equator of the particle and τ_0 can at low volume fractions of dispersoid be identified with the Orowan stress. Note the da is negative when moving the dislocation an increment dx in the forward direction. It is also emphasized that use of the A–W formalism implies the assumption of "local" climb; in view of the analysis by Arzt and Rösler [26], who show that local climb can in fact be stabilized by an attractive interaction, this assumption is not unreasonable.

The second energy term dW is due to the work done by the applied shear stress. It amounts to (A–W)

$$dW = 2T_M \cdot \frac{\tau}{\tau_0}\left(\frac{a}{\sqrt{r^2-h^2-a^2}} + \frac{\tau/\tau_0}{\sqrt{1-(\tau/\tau_0)^2}}\right)da \tag{6}$$

which is always negative. Thus the net energy change $dE = dU + dW$ is given by

$$dE = 2T_M\left[\frac{k}{\sqrt{1-\left(\frac{a}{r}\right)^2}} - \sqrt{1-(\tau/\tau_0)^2} + \frac{\tau}{\tau_0}\frac{a}{\sqrt{r^2-h^2-a^2}}\right]da. \tag{7}$$

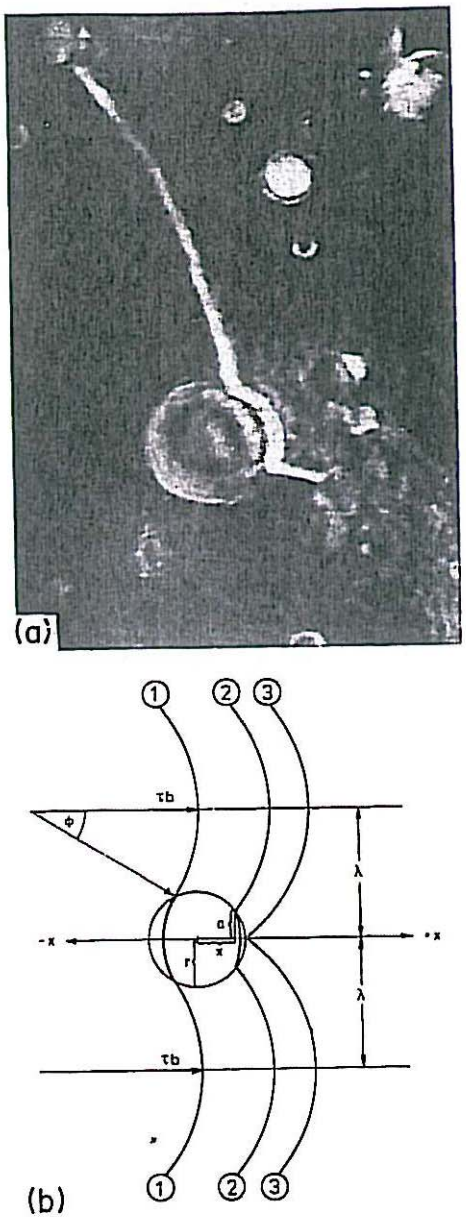

Fig. 1. (a) TEM micrograph showing a dislocation captured at the "detachment" side of a dispersoid particle: dispersion-strenthened superalloy MA 6000 after slow creep deformation, weak beam micrograph from Schröder and Arzt [21]. (b) Schematic illustration of the dislocation geometry during climb (1) and detachment (2, 3) after Arzt and Wilkinson [25].

By setting $dE = 0$ one obtains an implicit equation for the equilibrium position a_{eq} (or x_{eq} respectively) at a given stress τ/τ_0. The numerical solutions presented by A–W have a simple analytical form for $h = 0$

$$\frac{x_{eq}}{r} = k \cdot \sqrt{1-(\tau/\tau_0)^2} + \frac{\tau}{\tau_0}\sqrt{1-k^2} \tag{8}$$

and

$$a_{eq} = \sqrt{r^2 - x_{eq}^2}. \tag{9}$$

These equations, which are strictly valid only for $h = 0$, will be used further as an approximation in

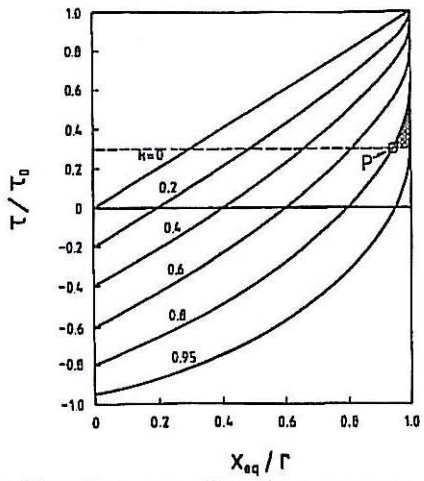

Fig. 2. Plot of the normalized shear stress τ/τ_0 vs the equilibrium dislocation position x_{eq}/r for different values of the relaxation parameter k, in the limiting case of the glide plane intersecting a spherical particle at its equator ($h = 0$). Shaded area is proportional to the activation energy for dislocation detachment at a stress τ which is below the athermal detachment threshold (for $k = 0.8$).

order to retain analytic tractability. Equation (8) is plotted in Fig. 2 for different values of the relaxation parameter k. The maximum stress is always obtained at the point of dislocation detachment from the particle ($x_{eq} = r$) and is equal to

$$\tau_d = \tau_0 \cdot \sqrt{1 - k^2} \tag{10}$$

as was already found by A–W. τ_d will henceforth be referred to as the "athermal detachment stress" because at this stress level thermal activation is not necessary to detach the dislocation from the particle. When however the applied stress is smaller than τ_d the dislocation will reach an equilibrium position at the particle back defined by equation (8), e.g. the point marked "P" in Fig. 2 (for $k = 0.8$). A finite activation energy E_d (corresponding to the shaded area in Fig. 2) has then to be supplied to enable dislocation detachment.

E_d is calculated by integrating equation (7)

$$E_d = \int_{a_{eq}}^{0} \frac{dE}{da}\, da = 2T_M \cdot r \left[\sqrt{1 - (\tau/\tau_0)^2} \times \frac{a_{eq}}{r} + \frac{\tau}{\tau_0}\left(\sqrt{1 - \left(\frac{a_{eq}}{r}\right)^2} - 1 \right) - k \cdot \arcsin\left(\frac{a_{eq}}{r}\right) \right]. \tag{11}$$

†The activation energy derived here for spherical particles is significantly smaller than that for cuboidal particles oriented with the sidefaces parallel to the direction of dislocation motion [26]. It is an artefact of the latter geometry that $2a_{eq}$ equals the particle size independent of k and τ/τ_d, which leads to a gross overestimation of the activation energy, especially at high values of k and τ/τ_d.

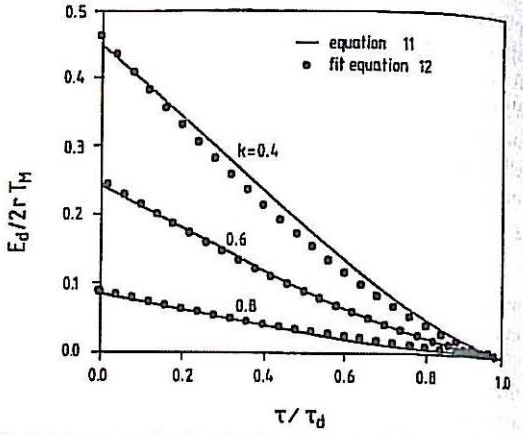

Fig. 3. The normalized activation energy $E_d/2T_M r$ vs τ/τ_d for different values of k. The analytical solution [equation (11)] is compared with the fit equation 12.

Note that E_d scales with the particle radius r since the terms in the square brackets are independent of r.

A convenient approximation for equation (11) was obtained in the following way. In Fig. 3 the normalized activation energy $E_d/2rT_M$ is plotted vs τ/τ_d for different relaxation parameters k. As required, E_d become zero for $\tau \to \tau_d$. The stress dependence of the activation energy turns out to be well approximated by

$$E_d = 2T_M \cdot r \cdot A \cdot (1 - \tau/\tau_d)^{3/2} \tag{12}$$

for $k \geqslant 0.4$ (Fig. 3); as will be shown later, k-values in real systems are typically greater than 0.7. The factor A is a function of k and is well fitted by (Fig. 4)

$$A = (1 - k)^{3/2}. \tag{13}$$

With $T_M \approx Gb^2/2$ one finally obtains the following expression for the detachment activation energy

$$E_d = Gb^2 \cdot r \cdot [(1 - k) \cdot (1 - \tau/\tau_d)]^{3/2}. \tag{14}$$

Note that this equation differs in form from the expression derived previously ([26], equation A5) for detachment from cuboidal particles†. It is similar to the activation energy of the Orowan process [13], with the exception that the particle radius r appears here instead of the particle spacing in the Orowan case. This difference, which can be large at low volume fractions, explains why thermal activation of the Orowan process fails to give the correct temperature dependence of the creep strength in dispersion hardened materials. The detachment process, by contrast, is associated with such low activation energies that consideration of thermal activation does become important. This is also qualitatively clear from the shape of the stress–distance profiles in Fig. 2. The steep slopes near the points of detachment lead to considerable reductions of the detachment stress when thermal energy (proportional to the shaded area under the curve) is supplied. As will be shown

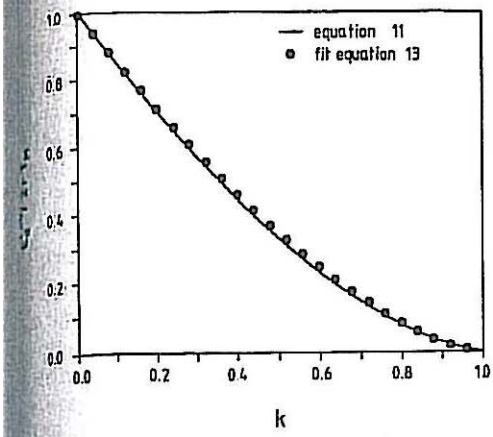

4. The normalized activation energy $E_d/2T_M r$ at $\tau = 0$ the relaxation parameter k. The analytical solution equation (11)] is compared with the fit equation (13).

Section 5, this concept can quantitatively explain creep strengths of several dispersion strengthened terials.

3. THE NEW CREEP EQUATION

Assuming that thermally activated dislocation de- chment from the particle is the rate controlling echanism in dispersion strengthened alloys and that climb process can be regarded as sufficiently pid, the rate equation for creep can now be written an Arrhenius expression

$$\dot{\epsilon} = \dot{\epsilon}_0 \cdot \exp\left(-\frac{E_d}{k_B T}\right) \tag{15}$$

here $\dot{\epsilon}_0$ is a reference strain rate. The reference strain e $\dot{\epsilon}_0$ may be estimated by applying nucleation eory [27]: the probability that the dislocation has ched the critical configuration (i.e. the point of achment x_k in Fig. 5) is given by the exponential m. Thus the frequency ν with which a dislocation detached from the particle, by moving from x_k to $_{+1}$ under absorption of a vacancy, is

$$\nu = \nu_{k,k+1} \cdot \exp\left(-\frac{E_d}{k_B T}\right) \tag{16}$$

here $\nu_{k,k+1}$ is the frequency of vacancy absorption

$$\nu_{k,k+1} = \frac{n}{2} \cdot \nu_0 \cdot \exp\left(-\frac{Q_n}{k_B T}\right) \cdot \exp\left(-\frac{Q_m}{k_B T}\right). \tag{17}$$

ere ν_0 is the atomic frequency and n the number next-nearest neighbour sites in the matrix lattice. and Q_m are the activation energies for vacancy cleation and migration, respectively. The factor $2)\exp(-Q_n/k_B T)$ is equal to the probability that one of the next-nearest neighbour sites is occupied by a vacancy, and $\nu_0 \cdot \exp(-Q_m/k_B T)$ scribes the frequency of successful jumps. oting that the diffusion coefficient is given by

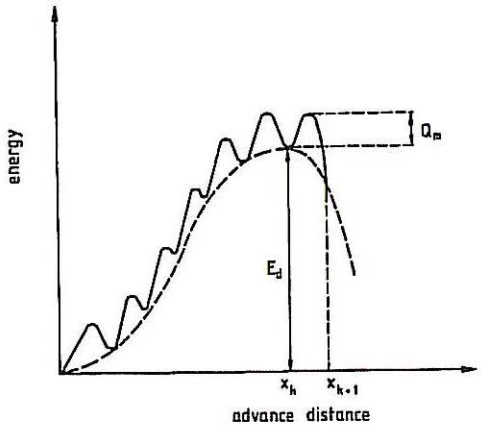

Fig. 5. Schematic energy barrier for detachment of a climbing dislocation from an attractive particle. (E_d; detachment energy due to attractive particle–dislocation interaction, Q_m: activation energy for vacancy migration).

$D_v = 1/6 \cdot n \cdot b^2 \cdot \nu_0 \cdot \exp(-(Q_n + Q_m)/k_B T)$ [28], one obtains

$$\nu = \frac{3D_v}{b^2} \cdot \exp\left(-\frac{E_d}{k_B T}\right). \tag{18}$$

Assuming that the time it takes to move a dislocation between the particles is negligible, the strain rate is connected with the detachment frequency ν by

$$\dot{\epsilon} = \rho \cdot 2\lambda \cdot \nu \cdot b \tag{19}$$

where ρ is the density of mobile dislocations and 2λ is taken as the mean free path between the obstacles. Combining the last two equations gives the final result

$$\frac{\dot{\epsilon}}{D_v} = \frac{6 \cdot \lambda \cdot \rho}{b} \cdot \exp\left(-\frac{Gb^2 r \cdot \left[(1-k)\left(1-\frac{\sigma}{\sigma_d}\right)\right]^{3/2}}{k_B T}\right). \tag{20}$$

Thus the reference strain rate defined in equation (15) may be identified as $\dot{\epsilon}_0 = 6D_v \cdot \lambda \cdot \rho / b$. The normalized shear stress τ/τ_d has been replaced by the normalized engineering stress σ/σ_d; σ_d is given by $\sigma_d = M \cdot \tau_d$ where M is the appropriate Taylor factor (or reciprocal of the Schmid factor for single crystals). For further analysis we use an "average" radius in equation (20), e.g. $(\pi/4)$ times the radius of spherical particles ($\pi/4$ accounts approximately for the statistical distribution of the intersect height), or a characteristic dimension for non-spherical particles.

As opposed to the empirical equation (1), this creep equation does not contain a "true" threshold stress. It is also important to note that equation (20) ceases to be applicable at very small stresses; fluctuations of the dislocation in the reverse direction would have to be taken into account in order to rule out the prediction of a finite strain rate at zero stress. This case however never becomes important in the analysis of dispersion strengthened materials (see section 5).

4. FORMAL ASPECTS OF THE CREEP EQUATION

Equation (20) represents a new constitutive equation for creep in dispersion strengthened materials. Like any equation treating dislocation creep, it can apply strictly only in the absence of additional deformation mechanisms, such as diffusional creep, damage accumulation etc., which can change the stress and the temperature dependence of the creep rate. A rigorous description of the creep behaviour can therefore be expected only for single-crystal or coarse-grained materials (see Section 5). In fine-grained alloys the discrepancy between experimental and theoretical creep rates can shed light on the relative contribution of grain boundary processes; one such example will also be analyzed below. But before turning to practical applications of the creep equation, we will discuss some general features and theoretical implications of equation (20).

4.1. The significance of the relaxation factor k for the creep strength

The exponential term reflects the fact that dislocation detachment is thermally activated, with an activation energy which is both dependent on the Orowan stress and the strength of the attractive interaction between dislocation and dispersoid particle, which in turn is measured by k. Thus the creep strength should not only be determined by the parameters of the particle distribution (particle diameter, volume fraction) as in Orowan-type models but also by the interfacial properties of a given particle–matrix combination. The relaxation factor k appears as a new important material parameter. Its magnitude can be expected to depend upon some interfacial properties but cannot yet be derived from first principles. Low values of k, which signify a strong particle–dislocation attraction [see equation (3)] are essential to the attainment of good creep properties. Note that the influence of the k-factor in equation (20) is in fact two-fold since the athermal detachment stress σ_d is by itself a function of k [equation (10)].

The effect of k is illustrated in Fig. 6 where the normalized strain rate $\dot{\epsilon}/\dot{\epsilon}_0$ is plotted against the normalized stress σ/σ_d for different values of k. It appears that $k \approx 0.9$ is a critical value: below this value the creep behaviour is "threshold"-like in the sense that the stress exponent is very high and a high creep strength is retained down to insignificantly small strain rates. The apparent stress exponent is obtained by differentiation of equation (20). Neglecting the stress dependence of the dislocation density in the pre-exponential factor, we get

$$n_{app} = \frac{d \ln \dot{\epsilon}}{d \ln \sigma} = \frac{3}{2}\frac{Gb^2 r}{k_B T}(1-k)^{3/2}(1-\sigma/\sigma_d)^{1/2}\cdot\sigma/\sigma_d. \quad (21)$$

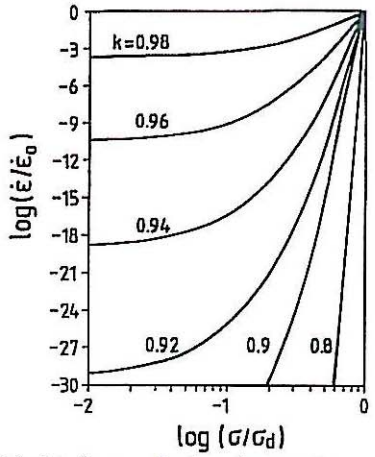

Fig. 6. Calculated normalized strain rate $\dot{\epsilon}/\dot{\epsilon}_0$ as a function of the normalized stress σ/σ_d for various values of the relaxation factor k [equation (20)].

This stress exponent is almost independent of stress since $(1-\sigma/\sigma_d)^{1/2}\cdot\sigma/\sigma_d$ varies only slowly with stress for $0.2 \leqslant \sigma/\sigma_d \leqslant 0.9$. Equation (20) is then equivalent to the usual power-law creep equation [11] with a very high stress exponent. The ability to predict a stress exponent which is approximately constant over several orders of magnitude in strain rate is a particular formal advantage of equation (20) over equation (1) when fitting actual creep data.

The creep characteristics change drastically when the interaction strength decreases. For $k \geqslant 0.9$ the creep strength degrades significantly with decreasing strain rate, which results in low values of the stress exponent n (Fig. 6). Normally one would tend to attribute such a creep behaviour, which is totally at variance with a "threshold"-like behaviour, to the onset of alternative creep processes such as diffusional creep or to microstructural instabilities. Fig. 6 illustrates that this need not necessarily be the case, but thermal activation of the dislocation detachment can in itself produce such a behaviour. As an example, the creep behaviour of a rapidly solidified alloy (Fig. 11 below) will be discussed in Section 5.

When the attractive interaction vanishes ($k \to 1$), the detachment barrier disappears too. Then the strengthening mechanism is reduced to the "climb effect", which at low volume fractions is much less efficient: the particles simply exert a back stress σ_b on moving dislocations and the creep kinetics is similar to that of the particle free material under an effective stress $\sigma_{eff} = \sigma - \sigma_b$ [29–31]. The back stress is proportional to the applied stress and can be associated with the increase of line length necessary for dislocation climb to occur [18]. At higher volume fractions, the climb process itself becomes rate-controlling, as recently analysed by Rösler and Arzt [19]. In both cases low stress exponents of about 4–6 are predicted, which is in qualitative agreement with experimental creep data for precipitation hardened alloys [29–31].

4.2. A method for determining the relaxation factor k from creep data

For the development of high temperature alloys the ability to predict the value of k on theoretical grounds would be highly desirable. Apart from the qualitative statements above this does not seem to be possible at present since too little is known about the nature of the particle–matrix interfaces in different systems. Thus time-consuming creep tests have to be conducted over a wide range of stresses and temperatures before the creep properties of a given system can be assessed.

A method for estimating k with little experimental expense can now be developed with the aid of equation (20). The following relationship is obtained by differentiation with respect to temperature

$$\frac{\sigma}{\sigma_d}=\left(\frac{3(Q_{app}-Q_v)}{2RT\cdot n_{app}\cdot\left(1-\frac{\partial G}{\partial T}\frac{T}{G}\right)}+1\right)^{-1} \tag{22}$$

where Q_v is the activation energy for vacancy diffusion and

$$Q_{app}=\left(\frac{\partial \ln \dot\epsilon}{\partial T}\right)_{\sigma/E}\cdot RT^2 \tag{23}$$

is the apparent activation energy evaluated at constant σ/E. [When the apparent activation energy has been obtained at constant σ, instead, the term $(n_{app}RT^2/G)\cdot(dG/dT)$ has to be subtracted before insertion in equation (22).]

An expression for k is obtained from equation (21)

$$k=1-\left(\frac{2k_BT}{3Gb^2r}\cdot\frac{n_{app}}{(1-\sigma/\sigma_d)^{1/2}\cdot\sigma/\sigma_d}\right)^{2/3}. \tag{24}$$

Inserting equation (22) in (24) now leads to an expression for k which depends upon two experimentally accessible quantities, i.e. the apparent stress exponent n_{app} and the apparent activation energy Q_{app}. About 5 creep tests for at least two temperatures and stresses are necessary to get access to both quantities by simple graphical evaluation; in practice, the scatter can of course be greatly reduced by running more tests. Only the mean particle radius has to be known in addition. The evaluation of k in this way will be exemplified in Section 5.

4.3. The optimum particle size

A consequence of equation (20) which is of practical importance lies in the prediction of an optimum particle size at a given volume fraction f_v. The reason is that the activation energy E_d for detachment goes through a maximum as a function of r; physically this comes about because (i) the probability of thermally activated detachment is raised at small dispersoid particles, and (ii) larger particles are associated, at fixed volume fraction, with a lower Orowan stress and hence a smaller athermal detachment stress σ_d.

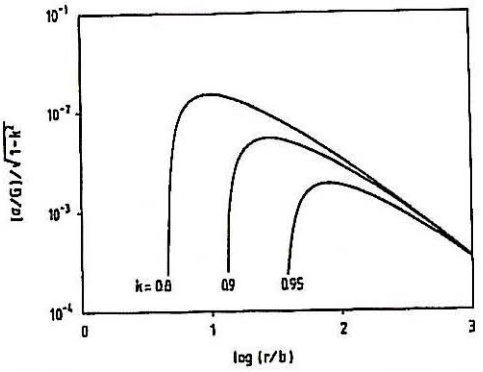

Fig. 7. The optimum particle size deduced from a plot of creep strength (for achieving $\dot\epsilon = 10^{-8}\,s^{-1}$) vs particle radius according to equation (25) for different values of k; $T = 673$ K, $M = 3$, $f_v = 0.05$, $\dot\epsilon_0 = 20\,s^{-1}$ (setting $D_v = 1.62\times10^{-15}\,m^2/s$, $2\lambda = 120$ nm, $\rho = 10^{13}\,m^{-2}$), $b = 2.86\times10^{-10}$ m, $G = 20$ GPa (data for aluminium from [50]). (The weak dependence of $\ln\dot\epsilon_0$ on λ is neglected in this plot.)

The creep strength σ as a function of r is obtained by inverting equation (20), using the identities $\tau_0 = 0.84\,Gb/(2\lambda)$ and $\lambda = (\pi/6f_v)^{1/2}\cdot r$

$$\frac{\sigma}{G}=0.84M\left(\frac{b}{r}\right)\left[1-\left(\frac{\ln(\dot\epsilon_0/\dot\epsilon)k_BT}{Gb^3}\frac{b}{r}\right)^{2/3}\times\frac{1}{1-k}\right]\left(\frac{3f_v}{2\pi}\right)^{1/2}(1-k^2)^{1/2}. \tag{25}$$

This functional dependence is displayed graphically in Fig. 7 for three different values of k, using material parameters of aluminium. It is interesting to note that not only is the creep strength predicted to rise with decreasing k, as expected, but also the optimum particle radius is shifted to smaller values. Below the optimum, a relatively sharp drop in creep strength occurs. Very small particles should therefore be inefficient barriers to the motion of dislocations at high temperatures and detachment will no longer be the rate-controlling step. Analytically, the optimum particle size is given by

$$\left(\frac{r}{b}\right)_{opt}=\left[\frac{5}{3(1-k)}\right]^{3/2}\left[\frac{\ln(\dot\epsilon_0/\dot\epsilon)k_BT}{Gb^3}\right]. \tag{26}$$

It is predicted to increase with rising temperature (at fixed $\dot\epsilon/\dot\epsilon_0$) and, less sensitively, with decreasing strain rate.

The creep strength maximum in the detachment model leads to a reduced sensitivity of the creep rate to particle coarsening. From an Orowan-type approach, the following particle size dependence results

$$\frac{d\ln\sigma}{d\ln r}=-\frac{\sigma_{th}}{\sigma} \tag{27}$$

which is approximately -1 at stresses near the "threshold stress". Thus the creep strength is predicted to double when the particle size is halved independent of current particle size.

By contrast, equation (25) leads to a weaker particle size dependence of the creep rate near the optimum (see also Fig. 7).

$$\frac{\mathrm{d}\ln\sigma}{\mathrm{d}\ln r} = \frac{2}{3}\cdot\frac{B}{(r/b)^{2/3}-B} - 1 \qquad (28)$$

with $B = [\ln(\dot{\epsilon}_0/\dot{\epsilon})k_B T/Gb^3]^{2/3}/(1-k)$.

As an example, consider a dispersion-strengthened nickel-based superalloy (MA 6000) with particle radius $r = 16.5$ nm [32] and $k = 0.93$ (see Section 5). Setting $\dot{\epsilon} = 10^{-8}\,\mathrm{s}^{-1}$, $\dot{\epsilon} = 10\,\mathrm{s}^{-1}$, $T = 1273$ K, and $G = 61$ GPa, equation (25) would predict a loss in creep strength by only about 28% on coarsening of the particles to twice their original size. Although such an effect has not been experimentally studied in detail, it seems to have been observed: Benjamin [33] reports that after doubling the interparticle spacing of the dispersoids in two nickel-base alloys, a loss of strength was found which was however "no where near 50%". Further support for the concept of an optimum particle size comes from detailed TEM observations [32, 34] which showed that dislocations did not adhere to dispersoids smaller than a critical size.

5. APPLICATION TO EXPERIMENTAL CREEP DATA

We will now proceed to compare the theoretical predictions of equation (20) with experimental data. In all cases, the unknown relaxation factor k is fitted to give optimum agreement with experiment. For a demonstration of the method, three different alloys are chosen: coarse-grained tungsten strengthened by a dispersion of bubbles, a coarse-grained, dispersion-strengthened superalloy and two fine-grained, dispersion-strengthened aluminium alloys.

5.1. Bubble-strengthened tungsten

The creep strength of tungsten wire filaments is commonly improved by doping with potassium, which forms a dispersion of vapor-filled bubbles at service temperatures. Creep data for such a material containing 0.3 vol.-% bubbles with mean diameter $2r \approx 9$ nm are plotted in Fig. 8 (from Wright [35]). While the bubble dispersion also stabilizes a coarse elongated grain structure and thus prevents grain boundary sliding, it was shown by Wright that the creep properties are controlled by the bubble–dislocation interaction. He assumed that the bubbles are cut by dislocations, which increases the surface energy. Since the climb process itself is fast [19] we consider dislocation climb over the bubble more likely because the additional surface energy is then avoided. Thus the above analysis should be applicable.

By linear regression one obtains an apparent stress exponent $n_{app} = 45$ at $T = 2800$ K and an apparent activation energy $Q_{app} = 1089$ kJ/mol (at $\sigma/E = 5.8 \times 10^{-4}$), which is about twice the activation

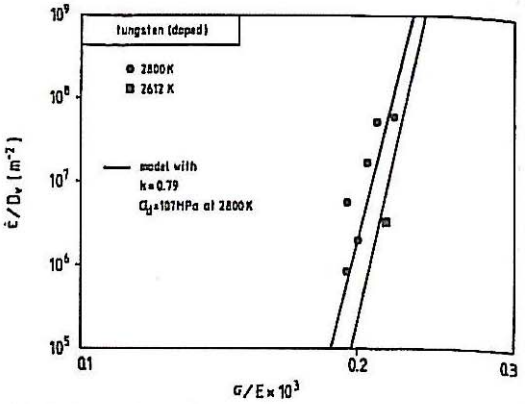

Fig. 8. Stress dependence of the normalized creep rate $\dot{\epsilon}/D_v$ for coarse-grained potassium doped tungsten (data from Wright [35]). The lines show the creep rate predicted by the model calculations ($k = 0.79$, $\sigma_d = 107$ MPa at 2800 K). Materials parameters used: $G = 160[1\text{-}0.38(T\text{-}300)/3683]$ GPa, $D_0 = 5.6 \times 10^{-4}\,\mathrm{m}^2/\mathrm{s}$, $Q_v = 585$ kJ/mol, $b = 2.74 \times 10^{-10}$ m [50], $\rho = 10^{13}\,\mathrm{m}^{-2}$, $2\lambda = 0.5\,\mu$m, $2r = 9$ nm [35].

energy for volume diffusion ($Q_v = 585$ kJ/mol). With the aid of equations (22) and (24) and using typical material parameters (see caption of Fig. 8), the relaxation parameter and the athermal detachment stress can be evaluated: $k = 0.79$ and $\sigma_d = 107$ MPa (at 2800 K). By inserting these values in equation (20), the creep rate was calculated; it is compared with the experimental data in Fig. 8. A very satisfactory agreement, both in absolute magnitude and in the stress dependence, is found.

An *a priori* estimate of the Orowan stress is also consistent with the analysis above. Following Wright [35], the average nearest neighbour spacing is about 0.5 μm, which takes the longitudinal alignment of the bubbles into account. Using the simplest expression for the Orowan stress $\sigma_0 = 0.84\,M\,Gb/(2\lambda)$ we obtain $\sigma_0 \approx 164$ MPa (at 280 K). Inserting $\sigma_d = 107$ MPa and $k = 0.79$ in equation (10) we obtain $\sigma_0 = 175$ MPa, which compares well with the above result.

The value of k obtained in the analysis also makes physical sense. The elastic interaction energy of a straight edge dislocation with a void of radius r is given by [36]

$$E_{el} = -\frac{5Gb^2r^3}{2\pi}\frac{1}{(7-5\nu)(1-\nu)} \times \frac{1}{r'^2}\cdot\left(1 - \frac{(1+6\nu-5\nu^2)}{5}\cdot\sin^2\Theta\right) \qquad (29)$$

where (r', Θ) are cylindrical coordinates and ν the Poisson ratio. Setting $\Theta = 0$ and assuming that the bubble is surmounted by climb (i.e. $r' = r$) one obtains $E_{el}/2r = -0.23\,T_M$ with $T_M \approx Gb^2/2$. Thus a 23% line tension relaxation corresponding to a k-value of 0.77 is expected at the bubble, independent of its diameter. This estimate, which of course ignores the core contribution, is in good agreement with $k = 0.79$ obtained from the creep data analysis.

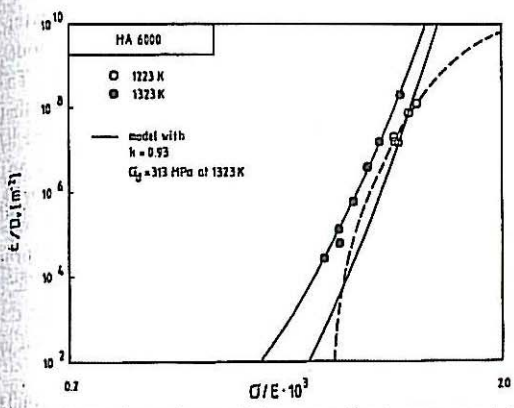

Fig. 9. Stress dependence of the normalized creep rate $\dot{\epsilon}/D_v$ for coarse-grained MA 6000 (data from Arzt and Timmins [38]). The creep rates calculated with equation (1) (dashed line) and equation (20) (solid line), with $k = 0.93$ and $\sigma_d = 313$ MPa at 1323 K, are compared with the experimental data. Further materials parameters used: $E = 170$ GPa at 1223 K and 155 GPa at 1323 K [37], $\nu = 0.34$, $D_0 = 1.9 \times 10^{-4}$ m²/s, $Q_v = 284$ kJ/mol, $b = 2.49 \times 10^{-10}$ m [50], $2r = 33$ nm [32].

5.2. Nickel base superalloys

Dispersion strengthened superalloys, which combine dispersion with precipitation hardening, are among the most promising metallic high temperature materials [37]. The alloy which has been studied in most detail is Inconel MA 6000, a Ni base superalloy strengthened in addition by yttria dispersoids. The creep properties available for this material are shown in Fig. 9 (data from [38]). Because of the highly elongated, coarse grain structure, the contribution of grain boundary processes to high temperature deformation is negligible in this alloy [39]. The apparent stress exponent is found to be $n_{app} = 23$, and the apparent activation energy of $Q_{app} = 546$ kJ/mol (at $\sigma/E = 1.16 \times 10^{-3}$) is again significantly higher than the activation energy for volume diffusion ($Q_v = 284$ kJ/mol for Ni in Ni).

Applying our analysis with the material data given in the caption of Fig. 9, we obtain $k = 0.93$ and $\sigma_d = 313$ MPa at 1323 K. The creep rate calculated with equation (20) is also shown in Fig. 9. Best fit was obtained by setting the pre-exponential factor $6\lambda\rho/b = 3.5 \cdot 10^{13}$ m^{-2} which differs by three orders of magnitude from the value calculated with $2\lambda \approx 100$ nm and $\rho \approx 10^{13}$ m^{-2}. This is no serious discrepancy because ρ is not well known and the pre-exponential varies sensitively with slight changes of σ_d owing to the high stress sensitivity of the creep rate.

As might have been expected, the relaxation factor k is significantly higher compared to doped tungsten, indicating that only about 7% of the dislocation line energy is relaxed at the dispersoids instead of about 21% at the bubbles in tungsten. As a consequence the apparent stress exponent is relatively low and the creep behaviour is less threshold-like. This is also illustrated in Fig. 9 where the creep rate calculated from equation 1 is included. As a "threshold stress", $\sigma_{th}/E = 0.76 \cdot 10^{-3}$ was obtained from linear back extrapolation (Lagneborg–Bergman plot [29] with $n = 4.6$) of the data points at 1323 K. The constant A was adjusted to fit one of the data points. The convex curvature resulting from the assumption of the simple threshold stress law equation (1) does not fit the data. In particular, it is evident that one would seriously overestimate the creep strength at low strain rates from that concept.

5.3. Aluminium alloys

Dispersion-strengthening has great potential for increasing the temperature capability of aluminium alloys. Promising fabrication routes for such alloys are mechanical alloying and rapid solidification. The creep properties of two typical representatives, both of which are fine-grained, are shown in Figs 10 and 11. Further results of a detailed study can be found elsewhere [6, 7, 40, 41].

A feature of the mechanically alloyed material Al–2.16 wt% C–0.80 wt% O, which contains both Al_2O_3 and Al_4C_3 as dispersoids, is the extremely high stress sensitivity ($n_{app} \approx 200$) at intermediate strain rates, which seems to be typical of carbide dispersion strengthened Al alloys (compare e.g. [4]). TEM investigations by Rösler [6] showed that creep in this regime is indeed controlled by the interaction of single dislocations with the dispersoids. At high strain rates $\dot{\epsilon}/D_v \geq 10^{12}$ m^{-2} the formation of dislocation networks is observed, indicating that the creep mechanism approaches that of the dispersoid-free matrix and is no longer directly determined by the particle

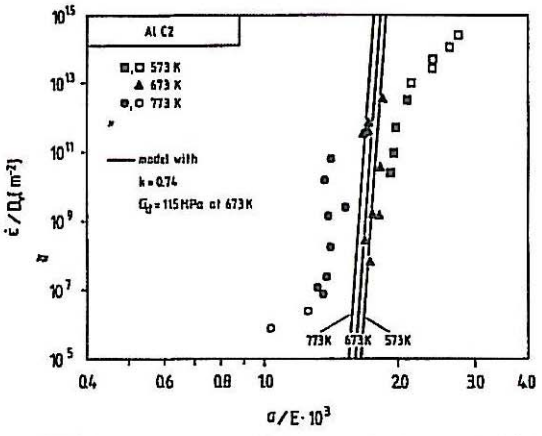

Fig. 10. Stress dependence of the normalized creep rate $\dot{\epsilon}/D_v$ for fine-grained Al–2.16 wt% C–0.80 wt% O (data from Rösler [6]). Solid symbols signify the region where particle-dislocation interaction controls the strength. The lines show the optimum predictions of the model ($k = 0.74$, $\sigma_d = 115$ MPa at 673 K). Failure of the model to give the correct temperature dependence points to substantial contributions of grain boundary processes (see text). Materials parameters used: $E = 72.2$, 61.5, 56.4, 50.0 GPa at room temperature, 573, 673 and 773 K, respectively [51], $G = 25.4$ [1-0.5(T-300)/933] GPa, $D_0 = 1.7 \times 10^{-4}$ m²/s, $Q_v = 142$ kJ/mol [50], $2\lambda = 101$ nm, $2r = 43$ nm [6], $\rho = 10^{13}$ m^{-2}.

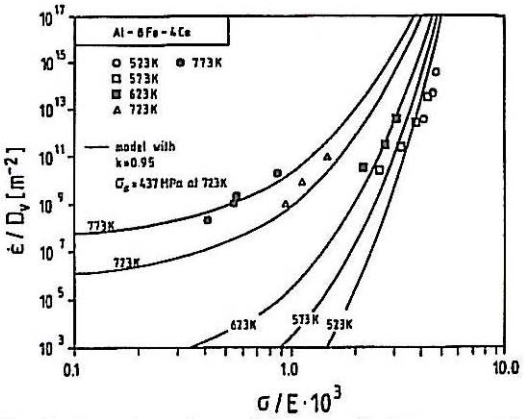

Fig. 11. Stress dependence of the normalized creep rate $\dot{\epsilon}/D_v$ for Al–8Fe–4Ce (data from Yaney and Nix [43]). The creep rates calculated with equation (20) are compared with the experimental data. Material parameters used: G, D_0, Q_v as in Fig. 10, $2r = 50$ nm, $\dot{\epsilon}_0 = 1.2 \times 10^{23}\,s^{-1}$, $\sigma_d = 577$ MPa at room temperature.

dispersion. The rapid degradation of the creep strength at the highest temperature and lowest creep rates occurs only in the fine-grained condition and may be attributed to the onset of grain boundary processes [6]. Thus the creep equation should be applied to the intermediate region, which extends over at least two orders of magnitude in strain rate (full symbols in Fig. 10).

Because this alloy has a submicron grain size, it is particularly instructive to apply equation (20) to the data. With the usual numerical analysis, one obtains from $n_{app} \approx 200$ and $Q_{app} \approx 1200$ kJ/mol a relaxation factor of $k = 0.75$. Agreement between theoretical and experimental data, however, can only be achieved by assigning a prohibitively high value to the pre-exponential factor ($\dot{\epsilon}_0/D_v = 10^{72}\,m^{-2}$ instead of $1.1 \times 10^{16}\,m^{-2}$, which would be obtained with $2\lambda = 101$ nm, $\rho = 10^{13}\,m^{-2}$). This discrepancy points to the fact that the strong temperature dependence of the creep rate cannot be explained on the basis of dislocation detachment.

Instead it is plausible that the rapid fall in creep strength with increasing temperature may be caused by an increasing contribution of grain boundary processes, which in conjunction with the steep stress dependence can give rise to the abnormally high activation energy. To remedy this situation, the value of k can instead be determined iteratively from equation (24) alone using the room temperature Orowan stress $\sigma_0 = 219$ MPa [6]. This procedure gives practically the same value as above: $k = 0.74$. With this value, and the known temperature dependence of the modulus, an athermal detachment stress of $\sigma_d = 115$ MPa at 673 K is obtained from equation (10). The pre-exponential factor which gives agreement with the creep data at 673 K is determined to be $\dot{\epsilon}/D_v = 3.3 \times 10^{18}\,m^{-2}$—in reasonable agreement with the value estimated above. The predictions with this consistent set of variables are plotted in Fig. 10.

It can be seen that while the temperature dependence is greatly underestimated by the model, the stress sensitivity is correctly reproduced. The following arguments support the contention that the remaining temperature dependence is caused by grain boundary effects: the model by Crossman and Ashby [42] confirms that creep-accommodated grain boundary sliding accelerates the creep rate in a way which leaves the stress sensitivity unaltered and produces a parallel off-set in creep strength; and first creep tests of recrystallized materials indicate that the strong temperature dependence is greatly reduced in coarse-grained specimens [41].

As a final example the creep data of a rapidly solidified Al-Fe–Ce alloy strengthened by intermetallic precipitates are shown in Fig. 11 (data from Yaney and Nix [43]). In this alloy the creep strength and the stress sensitivity decline strongly with increasing temperature. The authors have shown that this effect can probably not be explained by a thermal instability of the microstructure but have invoked a loss of particle strength instead. As is also seen in Fig. 11, both the complicated stress and temperature dependence of the creep behaviour can in fact be well described within the framework of our creep equation by setting $k = 0.95$, independent of temperature. This k factor points to a weak particle-dislocation interaction which allows considerable detachment by thermal activation at higher temperatures giving rise to the loss in creep strength. If the alloy is strengthened by additional oxide and carbide dispersoids introduced by mechanical alloying [44], this weakened effect is counteracted. A significantly reduced k value ($k \approx 0.90$) is obtained in this case.

6. DISCUSSION AND PRACTICAL CONCLUSIONS

In this paper we have presented a creep equation which is based on the mechanism of the particle-dislocation bypass process at high temperatures. The underlying assumption, which is supported by TEM and theoretical studies, is that incoherent particles in dispersion strengthened alloys exert an attractive interaction on dislocations. In order to make the problem tractable, only the detachment step, which is assumed to be rate-controlling, is considered. The resulting equation has been shown to be able to explain the creep behaviour of coarse-grained materials well, provided the interaction factor k is adjusted to give good agreement. A particular feature is that the stress as well as the temperature dependence of the creep rates, both of which are usually "abnormally" strong in the light of previous models, can be reproduced.

The new variable, k, is not merely a fit factor but has a well-defined physical meaning and assumes reasonable values. As summarized in Table 2, it ranges from below 0.8 for doped tungsten and

Table 2. Parameters for alloys analysed

Alloy	d (nm)	k	σ_d^{RT} (MPa)	$\log(\dot{\epsilon}_0/D_v, \mathrm{m}^{-2})$
K-Tungsten	9	0.79	145	16.7
MA 6000	33	0.93	477	13.5
Al-(C, O)	43	0.74	147	18.5
Al-8Fe-4Ce	~50	0.95	593	23.1

Al-(Al_4C_3, Al_2O_3) to above 0.9 for a superalloy and a rapidly solidified aluminium alloy. In all of these cases (except the fine-grained Al alloys) good agreement between theory and experiment could be obtained by keeping *k fixed* for all temperatures. This fact is consistent with calculations [6] which show that the characteristic relaxation times of shear and hydrostatic stresses on incoherent particles are short compared to the "waiting" time of a dislocation at a dispersoid.

In general it appears that precipitation hardened alloys behave like materials without attractive interaction whereas dispersion strengthened alloys, produced e.g. by mechanical alloying, behave like materials with a strong attractive particle–dislocation interaction. An important difference between the two particle types is that precipitates, unlike particles dispersed by mechanical means, have to overcome a nucleation barrier and are thus forced to form low energy (i.e. strongly bonded) phase boundaries. Weakly bonded interfaces are however needed to allow for the relaxation of the dislocation stress field by atomic rearrangements and fast diffusion along the interface. This may be the reason why small precipitates appear to be less capable of relaxing the line energy than small dispersoids. In addition incoherency across the interface can lead to some degree of core spreading once the dislocation has reached the particle. This would not be possible at a strongly bonded coherent interface where crystal periodicity has to be maintained. While the detailed understanding of the particle–dislocation interactions at high temperature is certainly not far advanced, it thus appears that on the basis of a varying degree of interfacial bond strength and of particle coherency the creep behaviour of the whole class of particle strengthened materials may be consistently understood. This in itself may constitute a possibly important advance over climb theories for which the type of interface does not play a role.

Despite these achievements some qualifications are in order: first, it must be remembered that in deriving the activation energy for dislocation detachment some simplifications were made (e.g. sphericals particles with equatorial glide planes) and second-order effects (e.g. self interaction of dislocation arms, statistics of particle distribution) were neglected; special particle shapes with re-entrant corners may well lead to different results as climb may then become rate-controlling (e.g. [45]).

The second qualification concerns the way in which fitting of the theory to experimental data is performed; because the creep strength and its temperature dependence vary sensitivity with k, the value of k extracted from the creep data, conversely, does not depend critically on σ/σ_d and Q_{app} [equations (22) and (24)]. The important quantity is n_{app}/r, which can be subject to considerable error, especially when the creep data are highly stress-sensitive and exhibit experimental scatter; also the mean particle dimension r is not always well defined. Obviously, in view of these possible inaccuracies, the relaxation factors k evaluated in this way should never be taken at face value, but regarded as a relative figure-of-merit for a particular alloy.

Because of the high stress dependences involved, a slight error in σ/σ_d will however shift the creep rate values drastically, and therefore a slight variance of the pre-exponential factor should not be considered as failure of the model. Critical examination of numerical consistency of k, σ_d and $\dot{\epsilon}_0$ is however, absolutely necessary, because an equation of the form of equation (20) with "free" parameters would have great flexibility. The fact that such consistency could be obtained in the above examples suggest strongly that creep is in these cases (with exception of the fine-grained Al variant, Fig. 10) controlled by a dislocation detachment process.

The practical conclusions that can be drawn from our concepts are still vague but enticing. Given a certain useable volume fraction of dispersoid (which is limited by minimum ductility requirements), the creep equation predicts an optimum particle size (Section 4.3). The concept of an optimum particle size hinges on the assumption of dislocation detachment and cannot be derived from Orowan-type threshold stress models. In the latter case, the creep strength would be predicted to increase indefinitely for finer particle dispersions (at least so long as the particles do not become shearable, which can occur when they reach the size of a few atomic spacings). Equation (25) and Fig. 7 show clearly that, compared to increasing the volume fraction (which enters only as the square root), aiming at the optimum particle size is a more efficient way of improving the creep strength. Optimizing the particle size may therefore pose a worthwhile challenge to processing techniques such as mechanical alloying.

In developing new alloys, particular attention should be paid to the properties of the particle–matrix interface. As pointed out above, it stands to reason that a high degree of dislocation relaxation can only be achieved at an incoherent interface with a high specific energy. Along these lines it is to be expected that thermally stable bubbles should be the most effective barriers for the motion of dislocations

at high temperatures since the line energy relaxation should be maximal in this case. Thus the k value estimated in Section 5.1 as $k \approx 0.77$ seems to be the lowest attainable relaxation factor; this implies that the high temperature strength imparted by any particle dispersion cannot exceed about 60% of the Orowan stress [equation (10)].

It is interesting to note that according to our analysis carbide dispersoids in Al alloys are about equally efficient as pores. Circumstantial evidence seems to suggest that the ability of interfaces to attract dislocations at high temperatures may be related to *poor* bonding across that interface: carbide-strengthened Al alloys exhibit a strong asymmetry of the flow stress [46] and the creep strength [6, 41] with respect to the loading direction; at high temperature the strength is reduced considerably under tension compared to compression (whereas no asymmetry is observed at room temperature). This asymmetry has been attributed to carbide decohesion from the matrix under tension and thus points to poor interfacial bonding. This is consistent with our finding that carbides are more beneficial for creep strength than oxides, the latter of which do not give rise to this asymmetry effect.

Weakening of the interfacial bonding, which may seem a paradoxical objective at first sight, might be possible by segregation alloying or by pre-treatment of the dispersoid material, much like fibres are coated to optimize the interfacial properties in fibre-reinforced materials. It is, for example, known that Ni additions weaken the interfacial bonding of Al_2O_3 particles in Fe whereas Cr and Mo have the opposite effect [47, 48]. The chemical compositions of an alloy may therefore well influence the effectiveness of dispersoid particles at high temperatures.

A further possibility to influence interfacial bonding may lie in the processing route itself. Preliminary creep experiments on Fe-base alloys seem to indicate that internally oxidized materials are less creep-resistant than their mechanically alloyed counterparts with similar composition and microstructure [49]. This may be expected from our model, since nucleation requirements and seclusion from atmospheric environment should lead to strong interfacial bonding in the case of internal oxidation. It remains to be seen whether these qualitative conclusions will hold and can eventually be put to technical use.

Finally, an important consequence concerns use of our creep equation for extrapolating creep data into regions where experimental data are not available. The shape of the curves in Fig. 6 suggests that only materials with highly attractive dispersoids ($k < 0.9$) show "threshold-like" behaviour. In general, uncritical use of a "threshold stress" concept may result in serious overestimates of the creep strength at low strain rates. This danger may be averted by using our model-based creep equation.

7. SUMMARY

1. A new creep equation has been developed which considers thermal activation of dislocation detachment from attractive dispersoid particles. This equation, which does not predict a "true" threshold stress, is shown to give good agreement with the hitherto "anomalous" creep behaviour of some dispersion-strengthened alloys in a coarse-grained condition. In contrast with earlier models, both the strong stress and temperature dependence of the creep rate can be explained.

2. The only fit parameter is the strength of the attractive particle–dislocation interaction (parameter k), which for incoherent dispersoids turns out to be superior over that of coherent precipitates. Optimum dispersion hardening would be expected from an array of stable pores.

3. The creep equation predicts the existence of an optimum particle size and suggests that there is room for obtaining stronger particle–dislocation interactions with new matrix–dispersoid combinations. It thus appears that there may be considerable scope for further alloy development.

4. Because it does not rest on a "threshold stress" assumption, the new creep equation can be used for "safer" extrapolations of the creep behaviour of dispersion-strengthened materials to low strain rates and high temperatures.

Acknowledgement—The research leading to this paper has been supported financially by the Bundesministerium für Forschung und Technologie under project number 03 M0010 E4.

REFERENCES

1. R. W. Lund and W. D. Nix, *Acta metall.* **24**, 469 (1976).
2. R. C. Benn and S. K. Kang, in *Superalloys 1984* (edited by M. Gell, C. S. Kortovich, R. H. Bricknell, W. B. Kent and J. F. Radavich), p. 319. T.M.S.-A.I.M.E., Warrendale, Pa (1984).
3. A. H. Clauer and N. Hansen, *Acta metall.* **32**, 269 (1984).
4. W. C. Oliver and W. D. Nix, *Acta metall.* **30**, 1335 (1982).
5. R. Petkovic-Luton, D. J. Srolovitz and M. J. Luton, in *Frontier of High Temperature Materials II* (edited by J. S. Benjamin and R. C. Benn), p. 73. INCO Alloys International, New York (1983).
6. J. Rösler, Doctoral dissertation, Univ. Stuttgart (1988).
7. E. Artz and J. Rösler, in *Dispersion Strengthened Aluminium Alloys* (edited by Y.-W. Kim and W. M. Griffith), p. 31. T.M.S., Warrendale, Pa (1988).
8. E. Arzt, *Res Mechanica* (1989). In press.
9. J. H. Gittus, *Proc. R. Soc.* **A342**, 279 (1975).
10. J. C. Gibeling and W. D. Nix, *Mater. Sci. Engng* **45**, 123 (1980).
11. A. K. Mukherjee, J. E. Bird and J. E. Dorn, *Trans. Am. Soc. Metals* **62**, 155 (1969).
12. E. Orowan, in *Symp. on Internal Stresses in Metals and Alloys*, p. 451. Inst. of Metals, London (1948).
13. P. Guyot, *Acta metall.* **12**, 941 (1964).
14. J. Weertman, *J. appl. Phys.* **26**, 1213 (1955).
15. M. F. Ashby, in *Proc. Second Int. Conf. on Strength of Metals and Alloys*, p. 507. Am. Soc. Metals, Asilomar, Ca (1970).

16. L. M. Brown and R. K. Ham, in *Strengthening Methods in Crystals* (edited by A. Kelly and R. B. Nicholson), p. 9. Elsevier, Amsterdam (1971).
17. R. S. W. Shewfelt and L. M. Brown, *Phil. Mag.* **35**, 945 (1977).
18. R. Lagneborg, *Scripta metall.* **7**, 605 (1973).
19. J. Rösler and E. Arzt, *Acta metall.* **36**, 1043 (1988).
20. V. C. Nardone and J. K. Tien, *Scripta metall.* **17**, 467 (1983).
21. J. H. Schröder and E. Arzt, *Scripta metall.* **19**, 1129 (1985).
22. R. S. Herrick, J. R. Weerman, R. Petkovic-Luton and M. J. Luton, *Scripta metall.* **22**, 1879 (1983).
23. D. J. Srolovitz, R. A. Petkovic-Luton and M. J. Luton, *Acta metall.* **31**, 2151 (1988).
24. D. J. Srolovitz, M. J. Luton, R. A. Petkovic-Luton, D. M. Barnett and W. D. Nix, *Acta metall.* **32**, 1079 (1984).
25. E. Arzt and D. S. Wilkinson, *Acta metall.* **34**, 1893 (1986).
26. E. Arzt and J. Rösler, *Acta metall.* **36**, 1053 (1988).
27. G. Schoeck, in *Dislocations in Solids* (edited by F. R. N. Nabarro), Vol. 3, p. 119. North Holland, Amsterdam (1980).
28. P. Shewmon, *Diffusion in Solids*. McGraw-Hill, New York (1963).
29. R. Lagneborg and B. Bergman, *Metals Sci.* **10**, 20 (1976).
30. B. Reppich, *Z. Metallk.* **73**, 697 (1982).
31. B. Reppich, H. Bügler, R. Leistner and M. Schütze, in *Creep and Fracture of Engineering and Structures* (edited by B. Wilshire and D. R. J. Owen), p. 279. Pineridge Press, Swansea, U.K. (1984).
32. J. H. Schröder, Doctoral dissertation, Univ. Stuttgart (1987).
33. J. S. Benjamin, Discussion contribution, in *Frontiers of High Temperatures Materials II* (edited by J. S. Benjamin and R. C. Benn), p. 120. INCO Alloys International, New York (1983).
34. E. Arzt, D. Elzey and J. H. Schröder, in *Advanced Materials and Processing Techniques for Structural Applications* (edited by T. Khan and A. Lasalmonie), p. 327. ONERA, Chatillon (1987).
35. P. K. Wright, *Metall. Trans.* **9A**, 955 (1978).
36. R. W. Weeks, S. R. Pati, M. F. Ashby and P. Barrand, *Acta metall.* **17**, 1403 (1969).
37. R. F. Singer and E. Arzt, in *High Temperature Alloys for Gas Turbines and Other Applications* (edited by W. Betz, R. Brunetaud, D. Coutsouradis, H. Fischmeister, T. B. Gibbons, I. Kvernes, Y. Lindblom, J. B. Marriott and D. B. Meadowcroft), p. 97, D. Reidel, Dordrecht (1986).
38. E. Arzt and R. Timmins, *Creep Properties of ODS Superalloys*, Overview Report, COST 501, (1988).
39. H. Zeizinger and E. Arzt, *Z. Metallk.* **79**, 774 (1988).
40. J. Rösler and E. Arzt, in *New Materials by Mechanical Alloying Techniques* (edited by E. Arzt and L. Schultz). DGM Informationsgesellschaft, Oberursel (1989). In press.
41. J. Rösler, R. Joos and E. Arzt (1989). To be published.
42. F. W. Crossman and M. F. Ashby, *Acta metall.* **23**, 425 (1975).
43. D. L. Yaney and W. D. Nix, *Metall. Trans.* **18A**, 893 (1987).
44. D. L. Yaney, M. L. Övecoglu and W. D. Nix, in Ref. [7], p. 619.
45. S. Goto, in *Creep and Fracture of Engineering Materials and Structures* (edited by B. Wilshire and R. W. Evans), p. 295. Inst. of Metals, London (1987).
46. M. Slesar, M. Besterci, G. Jangg, M. Miskovicova and K. Pelikan, *Z. Metallk.* **79**, 56 (1988).
47. H. F. Fischmeister, E. Navara and K. E. Easterling, *Metals Sci. J.* **6**, 211 (1972).
48. E. D. Hondros, *3rd Int. Conf. Science of Hard Materials*, Rhodes, Inst. Phys. Conf. Ser., No. 75, Chap. 2, p. 121 (1986).
49. R. Timmins and E. Arzt, unpublished results.
50. H. J. Frost and M. F. Ashby, *Deformation Mechanism Maps*. Pergamon Press, Oxford (1982).
51. W. Köster, *Z. Metallk.* **39**, 1 (1948).